Two dynamics modes in planar wire array Z pinch implosion

Sheng Liang(盛 亮)†, Wang Liang-Ping(王亮平), Wu Jian(吴 坚), Li Yang(李 阳), Peng Bo-Dong(彭博栋), and Zhang Mei(张 美)

Northwest Institute of Nuclear Technology, Xi'an 710024, *China*

(Received 11 September 2010; revised manuscript received 29 November 2010)

Two dynamics modes, named short ablation mode and long ablation mode, are observed in implosion experiments of planar wire array Z pinch on 'QiangGuang-I' facility utilizing an optical streak camera. The long ablation mode has a lagged trajectory compared with the short ablation mode. For shot 10035 in a short ablation mode, the initial time of K-shell radiation is consistent with the interaction time for ablation plasma arriving at the centre of wire array, while for shot 10038 in long ablation mode, the initial time of K-shell radiation is about 10 ns earlier. In the two modes, the partial ablation plasma could traverse the wire array plane and then collide in the centre to form a dense plasma column with a diameter of 2.2 mm for shot 10035 and 1.5 mm for shot 10038.

Keywords: ablation mode, imploding dynamics, planar wire array, Z pinch

PACS: 52.70.–m, 52.30.–q, 52.59.Qy **DOI:** 10.1088/1674-1056/20/5/055202

1. Introduction

The first planar wire array load design was used to study the ablation dynamics of wire and the formation of precursor plasma. The study of imploding planar wire array as a powerful radiation source has been performed on Zebra facility with a peak current of 1MA and rise time of 100 ns at the University of Nevada, Reno (UNR).[1,2] The long pulse experiments of planar wire array Z pinch performed on microsecond GIT-12 facility at the Institute of High Current Electronics at Tomsk (Russia) showed that the K-shell radiation was about twice that from the cylinder wire array.[3] Recently, experiments for tungsten planar wire array related to inertial confinement fusion (ICF), K-shell radiation of Al planar wire array, dynamics of wire array have been performed on Saturn accelerator with a peak current of 3 MA and rise time of 100 ns at Sandia National Laboratory.[4]

The dynamics of planar wire array is an important factor imposing on the instability control and radiation yield and is also a determining factor for rise time of the first X-ray pulse. The wire dynamics model (WDM) was developed to describe the dynamics behaviours of planar and nested wire arrays.[5] Some imploding parameters, such as implosion time and kinetic energy, were estimated using this model. In this model, the approximation of inelastic collision was used. The outer array could penetrate the inner array and stagnate in the centre of wire array in nested wire array imploding experiments.[6,7] Although the damp effect on the outer plasma moving in is stronger than the nested wire array load, the penetration phenomenon is directly observed in the implosion phase of planar wire array utilizing an optical streak camera in our imploding experiments for planar wire array on 'QiangGuang-I' facility with a peak current of 1.30 MA and rise time of 108 ns at Northwest Institute of Nuclear Technology. Two different dynamics modes, named the long ablation mode and the short ablation mode, observed in our experiments, will be discussed and compared with the wire dynamics model in this paper.

2. Introduction to wire dynamics model

If the return current path is represented by a conducting cylinder can, the dynamics equation can be written in the most compact form.[5,8] The acceleration of the n-th wire can be written as

$$\frac{\mathrm{d}^2 x_n}{\mathrm{d}t^2} = \frac{\mu_0}{2\pi}\frac{I_n}{\mu_n} \times \sum_{\substack{k=1 \\ k\neq n}}^{N} I_k \left(\frac{a^2 x_k - x_k^2 x_n}{\left|a^2 - x_n x_k\right|^2} - \frac{x_n - x_k}{\left|x_n - x_k\right|^2} \right), \quad (1)$$

†Corresponding author. E-mail: shengliang@tsinghua.org.cn

© 2011 Chinese Physical Society and IOP Publishing Ltd

where x_n is the position of the n-th wire, μ_0 is the vacuum permeability, μ_n is the wire mass per unit length, N is the total wire number in wire array, a is the radius of current return can ($a = 33.5$ mm for 'Qiang Guang-I' facility). Equation system (1) represents the mutual attraction between wires and the repulsion from return currents.

The approximation of inductive current partition is used in this paper. The current through each wire can be determined by Eqs. (2) and (3) to be

$$I_n \ln \frac{\left|a^2 - x_n^2\right|}{a r_{\rm w}} + \sum_{\substack{k=1 \\ k \neq n}}^{N} I_k \ln \frac{\left|a^2 - x_n x_k\right|}{a\left|x_n - x_k\right|} = \frac{2\pi\Lambda}{\mu_0}, \quad (2)$$

$$I = \sum_{n=1}^{N} I_n, \quad (3)$$

where $r_{\rm w}$ is the radius of wire and Λ is a constant that represents the value of the magnetic vector potential at the wire surface.

An approximation of inelastic collision will be used (see Ref. [5]). When the distance between two wires approaches some critical value, where $r_{\rm c} = 10 \cdot r_{\rm w}$ in this paper, they merge into a single wire. In a colliding stage, the mass and the momentum keep conserved. Under this assumption, the total wire number decreases in imploding phase.

3. Experimental results and discussion

The power exponent of piecewise sine function (Eq. (4)) is used to fit the load current I445 acquired by Rogowski coil with a radius of 22.5 cm (see Fig. 1). The K-shell radiation is measured by the Au cathode XRD, which is 1.19 m apart from the load, with a filter of 15 μm-polyethylene + 2.5 μm-mylar + 0.4 μm-Al. The soft X-ray radiation is measured by the Al cathode XRD, which is 2.20 m apart from the load, with a filter of 2.5 μm-mylar. The synch is used to obtain the time of streak image with respect to X-ray waveform. The Al planar wire array load parameters of shot 10035 and shot 10038 are as follows: wire number is 10, array width 8 mm, array length 20 mm, wire diameter 15 μm, wire mass 4.77 μg/cm and peak current 1.30 MA.

$$\frac{I}{I_0} = \begin{cases} \sin^2\left(\dfrac{\pi t}{2\tau_1}\right), & 0 < t \leq 60 \text{ ns}, \\ \sin\left(\dfrac{\pi t}{2\tau_2}\right), & 60 < t \leq 90 \text{ ns}, \\ \sin^6\left(\dfrac{\pi t}{2\tau_1}\right), & 90 < t \leq 108 \text{ ns}, \end{cases} \quad (4)$$

where $I_0 = 1.30$ MA, $\tau_1 = 108$ ns and $\tau_2 = 150$ ns.

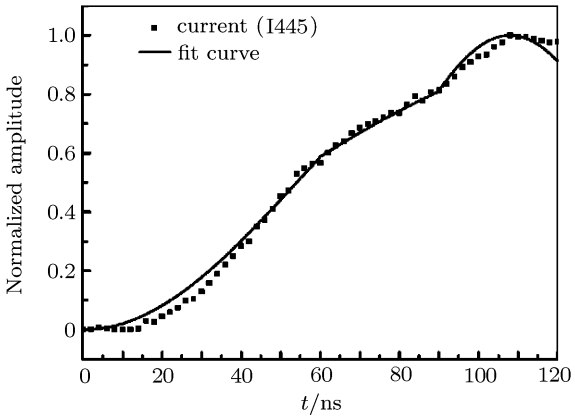


Fig. 1. Load current I445 waveform and its fitted curve.

The time relationship among streak camera image, X-ray, load current and synch is shown in Figs. 2 and 3. The optical length and the time of signal spent in the cable have been deducted.

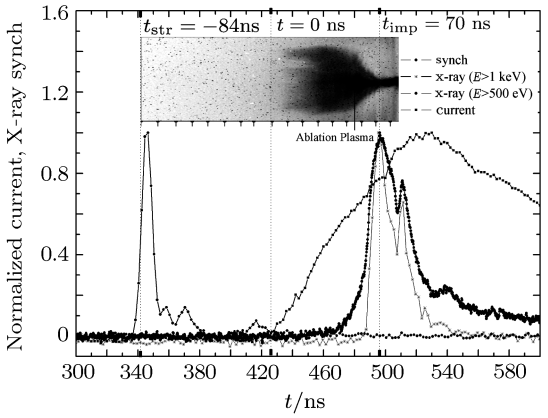


Fig. 2. Relationship among streak camera image, X-ray and current for shot 10035.

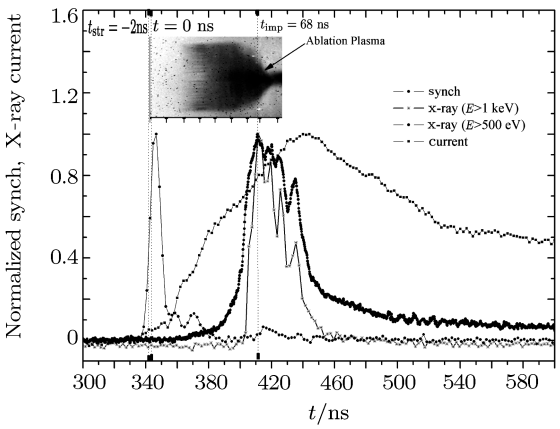


Fig. 3. Relationship among streak camera image, X-ray and current for shot 10038.

The time zero is determined by the intersection between the line connecting the 90% and 10% points of the current waveform and time axis. The implosion time is defined by the time interval between time zero and the time of X-ray peak. The ablation time is defined by the time interval between time zero and the time of beginning of the implosion.

In Figs. 2 and 3, the plasma implodes towards the centre of the wire array at $t = 40$ ns for shot 10035, while $t = 52$ ns for shot 10038. The ablation time of shot 10038 is about 12 ns longer than that of shot 10035. The synchronizing accuracy is less than 1 ns. The slit of the streak camera can only focus in a narrow region of load and the ablation along the axis is not uniform. The region of shot 10035 burns through earlier and subsequent implosion forms. Compared with the region of shot 10035, the region of shot 10038 has a lower ablating rate and the imploding plasma acts as trailing plasma, which is similar to the phenomenon of cylinder wire array Z pinch.[9,10] It is noted that the ablating plasma can traverse the semi-plane and collide in the centre of the wire array for both long ablation mode and short ablation mode. The dense plasma column forming in the array centre is similar to the precursor plasma column observed in the cylinder wire array Z pinch. Due to larger current passing through, the ablating rate of outer wire is higher than inner wire. The normalized current of the nth wire g_n is defined as

$$g_n = \frac{I_n \cdot N}{I}. \tag{5}$$

The current distribution through each wire during the whole stage, is computed by Eqs. (1)–(3) and shown in Fig. 4.

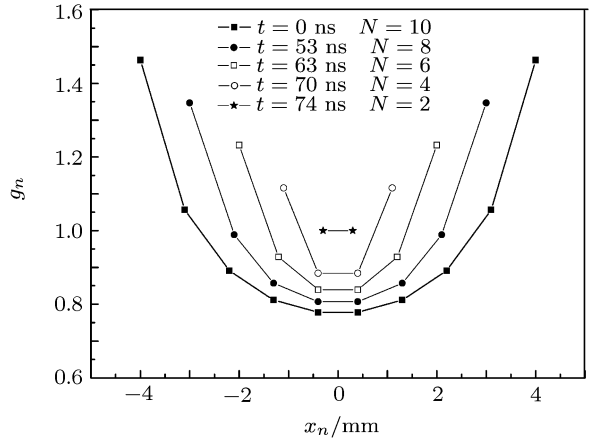


Fig. 4. Normalized current g_n according to the inductive current partition.

According to the inductive current partition, the normalized current of the outermost wire is about 1.9 times that of the innermost wire ($N = 10$). The ablating rate of the n-th wire is proportional to the square of the current,[11] that is to say, the majority of the ablating plasma comes from the outer wire. So the ablating plasma in planar wire array Z pinch will receive a strong resisting force when crossing the array plane compared with that produced in cylinder wire array. The time of the ablating plasma arriving at the array centre is about 15 ns before the X-ray peak for shot 10035, while 3 ns for shot 10038. The time difference with respect to X-ray peak is equal to the ablating time difference according to the streak images.

For shot 10035 with short ablation mode, the initial time of soft X-ray, which is consistent with the beginning time of implosion, is earlier than that of K-shell radiation corresponding to the time of ablating plasma arriving at the array centre. The implosion time deduced by both X-ray peak and streak image is 70 ns. The streak image of shot 10038 is obviously lagged compared with that of shot 10035. The implosion time is 68 ns obtained by X-ray peak, while 78 ns by streak image. The initial time of K-shell radiation is 9 ns earlier than the time of ablating plasma arriving at the array centre. The radiation pulse shapes are also quite different, 4 peaks for shot 10038 and double peaks for shot 10035.

The trajectories derived from the streak images and computed by WDM are shown in Fig. 5.

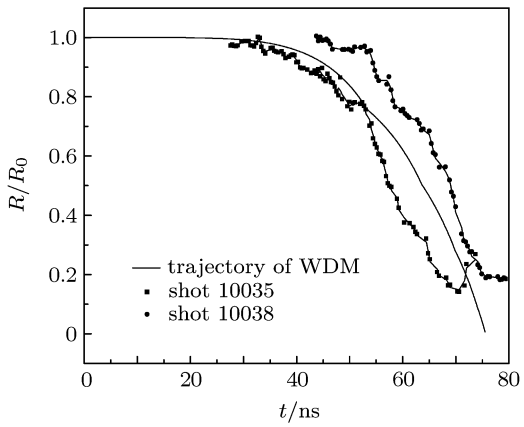


Fig. 5. The trajectories derived by streak image and computed by WDM.

The imploding velocity is 1×10^5 m/s for shot 10035 and 1.6×10^5 m/s for shot 10038. The implosion time computed by WDM is about 75.5 ns, with the total mass of wire array participating in the imploding phase. This time is shorter than that of the long ablation mode and longer than that of the short ablation mode, which indicates indirectly that only partial mass participates in the implosion phase. In order to prove this point further, the two-dimensional

(2D) optical framing image diagnostic system needs to be developed. The streak camera and framing camera should be accurately arranged in geometry, thereby fulfilling the requirement of the sub-mm ablating wavelength.

The diameter of the ablating plasma located on the array center decreases with time, see as Fig. 6.

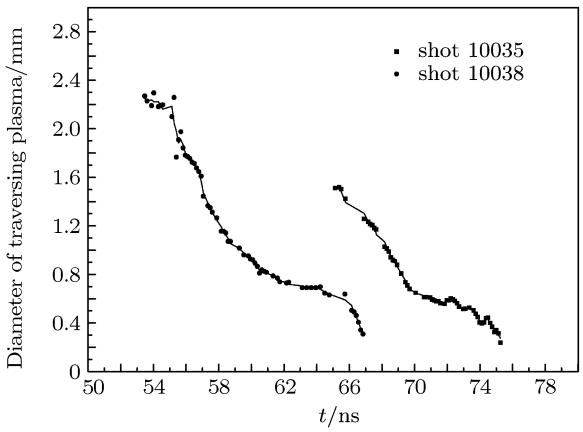


Fig. 6. Variation of diameter of ablating plasma located in the centre of array with time.

In Fig. 6, the initial diameter of ablating plasma is 2.2 mm for shot 10035 and 1.5 mm for shot 10038. The ablating plasma from outer wire continues colliding with the dense plasma column resulting in the mass accumulation in the array centre. The diameter will decrease if the momentum pressure is greater than the thermal pressure. In the long ablation mode, the plasma with some density may exist in the array centre before the ablating plasma arriving. The free length of plasma is in inverse proportion to the density, so the initial diameter of the long ablation mode is thinner than that of the short ablation mode.

4. Conclusions

Both the long ablation mode and the short ablation mode with different trajectories and radiation pulse shapes are observed in planar wire array Z pinch experiments. In the two modes, partial ablating plasma can traverse the array plane and collide in the array centre to form a dense plasma column. That is to say, there are both the colliding mode and the penetration mode in planar wire array Z pinch. The experimental results indicate that not all the array masses participate in the implosion phase. The phenomena observed in our experiments are beyond all the models known to us. In order to optimize the radiation shape and yield, the dynamics of planar wire array needs to be researched further. To develop a phenomenal model to describe the main physical stage of planar wire array Z pinch is one of the research subjects in our plan.

The streak camera has only one-dimensional spatial resolution along the slit. In order to diagnose the spatial modulation of ablation, an optical framing camera with 2D spatial resolution will be developed in our next experimental campaign. Some density diagnostic methods, such as laser probe and x-pinch probe, are also considered in our research plan.

References

[1] Kantsyrev V L, Rudakov L I, Safronova A S, Fedin D A, Ivanov V V, Velikovich A L, Esaulov AA, Chuvatin A S, Willianmson K, Quart N D, Nalajala V, Osborne G, Shrestha I, Yilmaz M F, Pokala S, Laca P J and Cowan T E 2006 *IEEE Trans. Plasma Sci.* **34** 2295

[2] Kantsyrev V L, Rudakov L I, Safronova A S, Esaulov A A, Chuvatin A S, Coverdale C A, Deeney C, Williamson K M, Yilmaz M F, Shrestha I, Ouart N D and Osborne G C 2008 *Phys. Plasmas* **15** 030704

[3] Shishlov A V, Chaikovsky S A, Fedunin A V, Fursov F I, Kokshenev V A, Kurmaev N E, Labetsky A Y, Oreshkin V I, Rousskikh A G and Zhidkova N A 2007 *34th IEEE International Conference on Plasma Science (ICOPS)* p. 467

[4] Jones B, Cuneo M E, Ampleford D J, Coverdale C A, Waisman E M, Vesey R A, Jones M, Esaulov A A, Kantsyrev V L, Safronova A S, Chuvatin A S and Rudakov L I 2007 *Sandia Report* **SAND2007** 6337

[5] Esaulov A A, Velikovich A L, Kantsyrev V L, Mehlhorn T A and Cuneo M E 2006 *Phys. Plasmas* **13** 120701

[6] Terry R E, Davis J, Deeney C and Velikovich A L 1999 *Phys. Rev. Lett.* **83** 4305

[7] Chittenden J P, Lebedev S V, Bland S N, Ciardi A and Haines M G 2001 *Phys. Plasmas* **8** 674

[8] Esaulov A A, Kantsyrev V L, Safronova A S, Velikovich A L, Cuneo M E, Jones B, Struve K W and Mehlhorn T A 2008 *Phys. Plasmas* **15** 052703

[9] Xu R K, Li Z H, Yang J L, Xu Z P, Ding N, Guo C, Jiang S L, Ning J M, Xia G X, Li L B, Song F J and Chen J C 2005 *Chin. Phys.* **14** 1613

[10] Cuneo M E, Sinars D B, Waisman E M, Bliss D E, Stygar W A, Vesey R A, Lemke R W, Smith I C, Rambo P K, Porter J L, Chandler G A, Nash T J, Mazarakis M G, Adams R G, Yu E P, Struve K W and Mehlhorn T A 2006 *Phys. Plasmas* **13** 056318

[11] Lebedev S V, Beg F N, Bland S N, Chittenden J P, Dangor A E, Haines M G, Kwek K H, Pikuz S A and Shelkovenko T A 2001 *Phys. Plasmas* **8** 3734